1972

Internal Relaxation in Short Chains Bearing Terminal Polar Groups

R. L. Jernigan, *National Institutes of Health*

INTERNAL RELAXATION IN SHORT CHAINS BEARING TERMINAL POLAR GROUPS

R. L. Jernigan

Physical Sciences Laboratory, Division of Computer Research and Technology, National Institutes of Health, Bethesda, Maryland,* and Department of Chemistry, University of California at San Diego, La Jolla, California

ABSTRACT

Dielectric relaxation can be described in terms of correlations between an initial dipole vector, $\underset{\sim}{\mu}(0)$, and its value at later times, $\underset{\sim}{\mu}(t)$. Here, this dipolar correlation function is averaged over all short chain configurations with a rotational isomeric state model. The time dependent behavior of molecular configurations is developed from rates for passing over internal rotational energy barriers. Configurational perturbations caused by electric fields are treated; such effects are determined to be usually small. The theory developed is applied to calculate the high frequency dielectric dispersion for members of the family of α,ω-dibromo-n-alkanes, $Br-(CH_2)_{n-1}-Br$ for n = 4 to 6. Distributions of internal relaxation times are reported. For the longer chains these distributions lead to depressed and slightly skewed Cole-Cole dielectric constant diagrams.

INTRODUCTION

Molecular details have been ignored in previous treatments of relaxation processes in chain molecules. In the highly successful Rouse-Zimm (1,2) model, the polymer molecule is divided into an unspecified number of free jointed Gaussian subunits. The relaxation of each subunit is assumed to behave as if it were a Hookean

*Present Address.

spring. The molecule is represented by a chain of beads connected with ideal springs. Frictional interactions with solvent occur only at beads. This representation succeeds in predicting observed low frequency relaxation behavior. Here a model is proposed to account for high frequency relaxation which is characterized by short range motions.

Resort to the devices of equivalent freely jointed chains and Gaussian distributions results in a considerable loss (3,4) of molecular information. In this paper a method for treating relaxation properties is set forth in which these artifices are avoided by using structural features previously employed to calculate equilibrium properties. These structural characteristics include fixed bond lengths, rigid bond angles and rotational isomers (3,4). Applications of these equilibrium theories have resulted in a fundamental understanding of a variety of electrical, geometric and optical properties (4) of polymers.

In the present model, transitions between molecular configurations occur by rotations about backbone bonds. High energy barriers to rotation permit a development of time dependent probabilities for rotational isomeric states. The rates of transitions about a given bond are assumed to be independent of states of neighboring bonds. However, extension to an interdependent model is straightforward within the present framework. The important neighbor interdependence of the equilibrium chain statistics (4) has been retained. Because frictional and hydrodynamic interactions are ignored, the treatment is appropriate only for isolated molecules. Applications are limited to small chain molecules or short polymer segments.

This equilibrium and non-equilibrium rotational isomeric state model has been applied to treat dielectric properties in several short chains of the homologous series of α,ω-dibromo-n-alkanes. These molecules were chosen because a previous treatment of their equilibrium mean square dipole moments $\langle\mu^2\rangle$ was available. After a short review of the theory of this property, the effect on the dipole moments, at equilibrium, of an external electric field is considered. Also discussed is the approximate perturbation of probabilities of individual molecular configurations resulting from the electric field. The development of time dependent configurational probabilities makes possible a direct calculation of the internal part of the dipolar auto-correlation function. It is also necessary to include an external contribution which corresponds to rotational diffusion of individual configurations. These external motions have been assumed to be independent of all internal motions. The complex dielectric constant is obtained directly from the dipolar autocorrelation function. Frequency and temperature dependences of the calculated dielectric dispersions are presented.

EQUILIBRIUM MEAN-SQUARE DIPOLE MOMENT (5)

Dipole moments of the class of molecules with polar groups at each terminus may be expressed as the sum of the two group moments, $\underset{\sim}{\mu}_1$, and $\underset{\sim}{\mu}_n$. For a fixed configuration, the molecular dipole moment is

$$\underset{\sim}{\mu} = \underset{\sim}{\mu}_1 + \underset{\sim}{\mu}_n \tag{1}$$

The values chosen for μ_1 and μ_n may be either the bond dipole moments or group moments so chosen as to also include induced effects in bonds adjacent to the polar bonds.

A right handed Cartesian coordinate system is assigned to every backbone bond. In the coordinate system based upon bond j, the x_j axis points along bond j. The y_j coordinate is chosen in the plane of bonds j-1 and j in a direction to form an acute angle with bond j-1. For such coordinate systems, the orthogonal transformation from the system j+1 to j is effected by

$$\underset{\sim}{T}_j = \begin{bmatrix} \cos\theta_j & \sin\theta_j & 0 \\ \sin\theta_j\cos\phi_j & -\cos\theta_j\cos\phi_j & \sin\phi_j \\ \sin\theta_j\sin\phi_j & -\cos\theta_j\sin\phi_j & -\cos\phi_j \end{bmatrix} \tag{2}$$

θ_j and ϕ_j are the bond angle supplement and rotational angle indicated for the alkane derivative shown in Figure 1. The angle ϕ_j is taken to be zero for the planar zigzag chain configuration.

The terminal bond dipole vectors of the hydrocarbon derivative shown in Figure 1 are given by

$$\underset{\sim}{\mu}_1 = \begin{bmatrix} \mu_1 \\ 0 \\ 0 \end{bmatrix} \quad \text{and} \quad \underset{\sim}{\mu}_n = \begin{bmatrix} -\mu_1 \\ 0 \\ 0 \end{bmatrix} \tag{3}$$

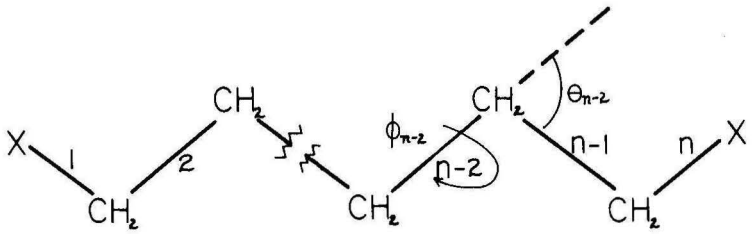

Figure 1. α,ω-dihalo-n-alkane chain in the planar form. An example of a rotational angle and bond angle supplement are shown. For the applications in this paper, X = bromine.

For a given configuration, the dipole moment is expressed here in the coordinate system of the first chain bond. Combination of Equations 1, 2 and 3 leads to

$$\underset{\sim}{\mu} = \underset{\sim}{\mu}_1 - \left(\prod_{j=1}^{n-1} \underset{\sim}{T}_j \right) \underset{\sim}{\mu}_1 \qquad (4)$$

The required mean-square dipole moment is obtained by squaring and averaging the last equation to give

$$\langle \mu^2 \rangle = 2\mu_1^2 - 2\underset{\sim}{\mu}_1^T \left\langle \prod_{j=1}^{n-1} \underset{\sim}{T}_j \right\rangle \underset{\sim}{\mu}_1 \qquad (5)$$

Angle brackets denote averages over all configurations accessible to the molecule and ^{T} indicates the transpose of the matrix to which it is attached.

Further structural details are required in order to perform the average indicated in Equation 5. Near equilibrium, bond lengths and bond angles may be assumed to be fixed. The distribution of configurations arises solely because of variations in the set of rotational angles $\{\phi\}$. Enumeration of the n-2 backbone rotational angles serves to specify a molecular configuration.

For the n-alkanes and numerous other molecules (4), the configurational energy has been found to exhibit three minima which lie near $\phi = 0°$, 120° and 240°. The positions of these minima are designated trans(tr), gauche$^+$(g+) and gauche$^-$(g-). For the n-alkane chains, the minima are deep and nearly symmetric; hence, it is valid to assume that all molecular configurations may be generated by permitting each of the rotational angles to independently assume each of the three rotational positions. This yields a total of 3^{n-2} configurations for a chain of n bonds. In n-alkane chains (6) the g+ and g- states possess an energy approximately 0.5 kcal mole^{-1} above the trans energy. In addition, high energy configurations are encountered when pairs of bonds assume rotational states of g+g or g-g+. This effect may be accounted for by choosing the configurational weights to be neighbor dependent. It is convenient to account for this dependence in a matrix of statistical weights,

$$\underset{\sim}{U}_j = \begin{bmatrix} 1 & \sigma & \sigma \\ 1 & \sigma & 0 \\ 1 & 0 & \sigma \end{bmatrix} \quad 2 < j < n-1 \qquad (6)$$

where $\sigma = \exp(-0.5/RT)$. The rows of $\underset{\sim}{U}_j$ index rotational states for bonds j-1 and the column index states for bond j in the order tr, g+ and g-.

Rotational energies about carbon-carbon bonds 2 and n-1 are different because the bond lengths C-X and C-C are different and because of different van der Waals radii for methylene and for X. For α,ω-dibromo-n-alkane chains treated here, the form of these matrices is

$$\underset{\sim}{U}_2 = \underset{\sim}{U}_{n-1} = \begin{bmatrix} 1 & 1 & 1 \\ 1 & 1 & 0 \\ 1 & 0 & 1 \end{bmatrix} \qquad (7)$$

The equilibrium partition function for these molecules is given by

$$Z = \underset{\sim}{J}^{*}\underset{\sim}{U}_2 \left(\overbrace{\prod_{j=3}} \underset{\sim}{U}_j \right) \underset{\sim}{U}_{n-1} \underset{\sim}{J} \tag{8}$$

which is the sum of weights for all configurations. The row and column matrices in Equation 8 are defined as

$$\underset{\sim}{J}^{*} = [1\ 0\ 0] \text{ and}$$

$$\underset{\sim}{J} = \begin{bmatrix} 1 \\ 1 \\ 1 \end{bmatrix}$$

This partition function is utilized in a straightforward manner to average the product of matrices $\underset{\sim}{T}$ in the r.h.s. of Equation 5

$$\left\langle \overbrace{\prod_{j=1}} \underset{\sim}{T}_j \right\rangle = Z^{-1} \left(\underset{\sim}{J}^{*} \otimes \underset{\sim}{I}_3\right) \| \underset{\sim}{T}_1 \| \overbrace{\prod_{j=2}} \left[\left(\underset{\sim}{U}_j \otimes \underset{\sim}{I}_3\right) \| \underset{\sim}{T}_j \|\right] \cdot \left(\underset{\sim}{J} \otimes \underset{\sim}{I}_3\right) \tag{9}$$

$\underset{\sim}{I}_3$ is the unit matrix or order 3; $\otimes$ represents the direct matrix product. We define the pseudo-diagonal matrix $\| \underset{\sim}{T} \|$ by

$$\| \underset{\sim}{T} \| = \begin{bmatrix} \underset{\sim}{T}(\phi=0°) & & \\ & \underset{\sim}{T}(\phi=120°) & \\ & & \underset{\sim}{T}(\phi=240°) \end{bmatrix}$$

Substitution of this result into Equation 5 yields an expression for the mean-square equilibrium dipole moment

$$\langle\mu^2(t=\infty)\rangle = 2\mu_1^2 - 2Z^{-1}\,\underset{\sim}{\mu}_1^T\,(\underset{\sim}{J}^*\otimes\underset{\sim}{I}_3)\,\|\underset{\sim}{T}_1\| \prod_{j=2}^{n-1}\,[(\underset{\sim}{U}_j\otimes\underset{\sim}{I}_3)\,\|\underset{\sim}{T}_j\|]\,(\underset{\sim}{J}\otimes\underset{\sim}{I}_3)\,\underset{\sim}{\mu}_1 \qquad (10)$$

Generally $\langle\mu^2\rangle$ will depend on the applied electric field or its residual influence after it has been removed. Here, t measures time after an initially applied field has been switched off; thus $t = \infty$ represents equilibrium.

Numerical calculations were carried out by Leonard, et al., (5) with this equation for the series of α,ω-dibromo-alkanes of different chain lengths at 25°. Effects of dipole-dipole interactions were also included. For chains longer than $Br-(CH_2)_5-Br$, agreement within about 5% of the experimental values was achieved by a choice of $\mu_1 = 1.90D$. A small dependence of $\langle\mu^2\rangle$ on temperature was computed which agrees with experiment. Inclusion of usually accepted small values for $u_{g+g-} = 0.02$ instead of the zeros in the 2,3 and 3,2 elements of $\underset{\sim}{U}_j$ raised calculated moments by less than 1%. All following results were calculated using Equations 8 and 10 with $\theta_j = 68°$, $\mu_1 = 1.90D$, and $\sigma = \exp(0.5/RT)$. In addition, dipole-dipole interactions have been ignored; previous calculations indicated their effect to always be less than about 5%. Also g+g- and g-g+ pairs have been excluded throughout.

EQUILIBRIUM MEAN-SQUARE DIPOLE MOMENT IN PRESENCE OF ELECTRIC FIELD

The molecular energy in an electric field which acts along the x axis is given by

$$E_F = E - \mu_x F - (\alpha_{xx}/2)F^2 \qquad (11)$$

where E is the internal energy in the absence of the field; F is the magnitude of the electric field. μ_x and α_{xx} represent the components of the dipole moment and the polarizability tensor in the direction of the field. This last term will be ignored because only polar molecules are treated here.

The partition function in the presence of an electric field is given by

$$Z_F = (8\pi^2)^{-1} \int \ldots \int \exp(-E_F/kT) \sin\chi \, d\chi \, d\psi \, d\rho \, d\{\phi\} \qquad (12)$$

where χ, ψ and ρ are the Euler angles and k is the Boltzmann constant. Substitution for E_F from Equation 11 and expansion of the exponential function $\exp(\mu_x F/kT)$ yields

$$Z_F = (8\pi^2)^{-1} \int \ldots \int \exp(-E/kT) \left[1 + \mu_x F/kT + \mu_x^2 F^2/(2k^2T^2) + \mu_x^3 F^3/(6k^3T^3) + \mu_x^4 F^4/(4!k^4T^4) + \ldots\right] \sin\chi \, d\chi \, d\psi \, d\rho \, d\{\phi\} \qquad (13)$$

The first term is identical to the field free partition function. Terms in odd powers of μ_x vanish. The result is

$$Z_F = Z \left[1 + (1/2) \langle\mu_x^2\rangle (F/kT)^2 + (1/4!) \langle\mu_x^4\rangle (F/kT)^4 + \ldots\right] \qquad (14)$$

Symmetry permits substitution of $\langle\mu_x^2\rangle = (1/3)\langle\mu^2\rangle$ and $\langle\mu_x^4\rangle = (1/9)\langle\mu^4\rangle$. Thus Equation 14 becomes

$$Z_F = Z \left[1 + (1/6) \langle\mu^2\rangle (F/kT)^2 + (1/216) \langle\mu^4\rangle (F/kT)^4 + \ldots\right] \qquad (15)$$

This equation expresses the field dependent partition function in terms of the field free partition function and a series in even powers of (F/kT). Coefficients in the series are proportional to the even field free moments of the dipole vector.

Approximate expressions for any desired property in the presence of the electric field may be obtained by averaging with the partition function in Equation 15. Only the mean-square dipole moment is treated here. Direct application of Equation 13 to obtain the requisite average yields

$$\langle\mu^2\rangle_F = (Z/Z_F)\ [\langle\mu^2\rangle + (1/2)\ \langle\mu^2\mu_x^2\rangle\ (F/kT)^2 + (1/4!)\ \langle\mu^2\mu_x^4\rangle\ (F/kT)^4 + \ldots] \qquad (16)$$

Introduction of the symmetry of components of the even dipole moments into Equation 16 gives

$$\langle\mu^2\rangle_F = (Z/Z_F)\ [\langle\mu^2\rangle + (1/6)\ \langle\mu^4\rangle\ (F/kT)^2 + (1/216)\ \langle\mu^6\rangle\ (F/kT)^4 + \ldots] \qquad (17)$$

Exact calculation of terms in this series beyond $\langle\mu^2\rangle$ is difficult but can be accomplished by methods presented in References 4 and 7. For short chains, these moments are obtained by explicit enumeration of all configurations, their associated dipole vectors and statistical weights.

Maximum values of the even dipole moments are obtained for a Gaussian distribution which corresponds to infinite chain length. In this case, the higher even moments may be replaced by powers of $\langle\mu^2\rangle$ with appropriate numerical coefficients.

$$\text{Maximum}(\langle\mu^{2j}\rangle) = [(2j+1)!/j!]\ (\langle\mu^2\rangle/6)^j \qquad (18)$$

Substitution of these expressions into Equations 15 and 17 results in the limiting expressions,

$$\langle\mu^2\rangle_F = (Z/Z_F)\ [\langle\mu^2\rangle + (5/18)\ \langle\mu^2\rangle^2\ (F/kT)^2 + (35/1944)\ \langle\mu^2\rangle^3\ (F/kT)^4 + \ldots] \quad (19)$$

and

$$Z_F = Z\ [1 + (1/6)\ \langle\mu^2\rangle\ (F/kT)^2 + (5/648)\ \langle\mu^2\rangle^2\ (F/kT)^4 + \ldots] \quad (20)$$

Substitution of Equation 20 into Equation 19 yields

$$\langle\mu^2\rangle_F = \langle\mu^2\rangle + (1/9)\ \langle\mu^2\rangle^2\ (F/kT)^2 - (2/243)\ \langle\mu^2\rangle^3\ (F/kT)^4 + \ldots \quad (21)$$

This Gaussian expression for $\langle\mu^2\rangle_F$ represents the maximum value obtainable for the normal range of values of F, T and $\langle\mu^2\rangle$. Values of $\langle\mu^2\rangle_F$ calculated for 1,4-dibromo-butane at 25° are presented in Table I. Results of calculations of the maximum value in Equation 21 are included as well as those calculated by the more exact series in Equations 15 and 17. Normally $\mu F \ll kT$; therefore, we conclude that only large fields will have significant effects on $\langle\mu^2\rangle_F$. Within the range of small effects, deviations of $\langle\mu^2\rangle_F$ from $\langle\mu^2\rangle$ may adequately be described by means of Equation 21.

$\langle\mu^2\rangle_F$ differs from $\langle\mu^2\rangle$ because an external electric field changes the probabilities of individual rotational states. The interaction between the electric field and the dipole moment decreases the total energy; therefore, the probabilities of configurations with large dipole moments are favored. The treatment below of probabilities of bond rotational states in the presence of an electric field closely follows the derivation presented by Abe and Flory (8) for bond state probabilities with chain stretching.

TABLE I

Effect of Electric Field on Dipole Moment of 1,4-dibromo-n-butane (25°)
($\langle\mu^2\rangle$ = 5.780D)

F/kT (Units of Debye^{-1})	$\langle\mu^2\rangle_F$ (Units of Debye^2) Eq. 17 with terms through $\langle\mu^4\rangle$	Eq. 17 with terms through $\langle\mu^6\rangle$	Gaussian Limit Eq. 21
0.03	5.784	5.784	5.784
0.06	5.793	5.793	5.794
0.09	5.809	5.810	5.812

Application of Equation 8 leads to an expression for the probability that bond i is in rotational state η,

$$p_{\eta;i} = Z_{\eta;i}/Z = Z^{-1} \underset{\sim}{J}^* \left[\overbrace{\prod_{j=2}^{i=1}} \underset{\sim}{U}_j \right] \underset{\sim}{U}'_{\eta;i} \left[\overbrace{\prod_{k=i+1}^{n-1}} \underset{\sim}{U}_k \right] \underset{\sim}{J} \quad (22)$$

where $\underset{\sim}{U}'_{\eta;i}$ is the matrix with two columns of zeros and the third column identical to the η^{th} column of $\underset{\sim}{U}_i$. By analogy with Equation 15, the statistical weight for bond i in rotational state η in the presence of the electric field is given by

$$Z_{\eta;i;F} = Z_{\eta;i} \left[1 + (1/6) \langle\mu^2_{\eta;i}\rangle (F/kT)^2 + (1/216) \langle\mu^4_{\eta;i}\rangle (F/kT)^4 + \ldots\right] \quad (23)$$

The moments in this equation bearing subscripts $\eta;i$ are calculated subject to the constraint that bond i remains in rotational state η.

Likewise, the probability that bond i is in rotational state η in the presence of an electric field is defined by

$$p_{\eta;i;F} = Z_{\eta;i;F}/Z_F \tag{24}$$

Substitution of Equations 23 and 15 into Equation 24, followed by division of the two series, yields

$$\begin{aligned} p_{\eta;i;F} &= (Z_{\eta;i}/Z)\ [1 + (1/6)\ (\langle\mu^2_{\eta;i}\rangle - \langle\mu^2\rangle)\ (F/kT)^2 + \ldots] \\ &= p_{\eta;i}\ [1 + (1/6)\ (\langle\mu^2_{\eta;i}\rangle - \langle\mu^2\rangle)\ (F/kT)^2 + \ldots] \end{aligned} \tag{25}$$

The factor $(\langle\mu^2_{\eta;i}\rangle - \langle\mu^2\rangle)$ in the correction term demonstrates the effect of η. If η produces a mean-square dipole moment $\langle\mu^2_{\eta;i}\rangle$ which is larger than the total field free moment, then $p_{\eta;i;F}$ will be larger than $p_{\eta;i}$. If, however, $\langle\mu^2\rangle$ is greater than $\langle\mu^2_{\eta;i}\rangle$, then state η is less probable in the presence of the electric field than in its absence.

It is convenient to define a coefficient of the average effect of the electric field on the probabilities of bond i. For a chain of length n this coefficient is defined to be

$$C(i,n) = (1/3) \sum_{\eta=tr,g+,g-} |\langle\mu^2_{\eta;i}\rangle - \langle\mu^2\rangle|/m_1^2$$

In Figure 2 the dependence of C(i,n) on n is shown for i=2 and i=3. Except for the very shortest α,ω-dibromoalkanes, C(i,n) is smallest for values of i nearest the middle of the chain. The zigzag character of the curves is a consequence of the bond geometry. The results depicted in Figure 2 indicate that the effect of the electric field upon bond rotational probabilities is usually largest for bonds nearest the bond dipoles.

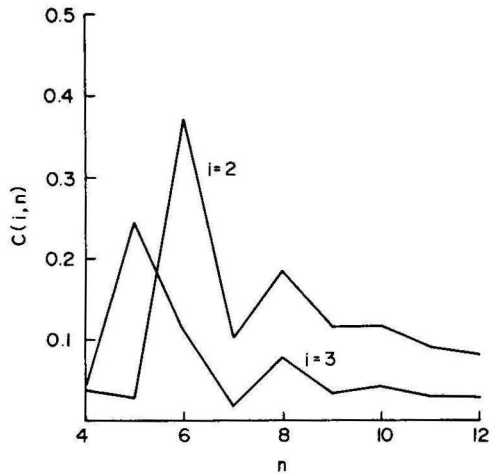

Figure 2. Relative average influence of an electric field on the rotational probabilities for the i^{th} bond in n bond α,ω-dibromo-n-alkane chains. Results are for 25°.

DIPOLAR TIME CORRELATION FUNCTION

The frequency dependence of the dielectric constant is directly related (9-13) to the dipolar time correlation function,

$$\Phi(\tau+t) \equiv \langle \underset{\sim}{\mu}(\tau) \cdot \underset{\sim}{\mu}(\tau+t) \rangle / \langle \mu^2(\tau) \rangle \qquad (27)$$

For a stationary process the origin in time is arbitrary so that

$$\Phi(\tau+t) = \Phi(t) \equiv \langle \underset{\sim}{\mu}(0) \cdot \underset{\sim}{\mu}(t) \rangle / \langle \mu^2(0) \rangle \qquad (28)$$

This function is properly normalized so that $\Phi(t = 0) = 1$ and $\Phi(t = \infty) = 0$. Decay of $\Phi(t)$ is assumed to occur by two independent processes, external rotational diffusion of the whole molecule and

internal relaxation by transitions between rotational isomeric configurations. Thus the total dipolar time correlation function is expressed as

$$\Phi(t) = \Phi_{int}(t) \exp(-t/\tau_{rot}) \qquad (29)$$

where τ_{rot} is the rotational relaxation time of a rigid body with dimensions equivalent to the average molecular dimensions.

Hoffman (14) proposed a mechanism of rotational barriers to explain dielectric relaxation in solid polymers. In his model barriers arise because of intermolecular interactions. In the treatment for isolated molecules which follows, intramolecular interactions are the source of rotational barriers.

Calculation of Φ_{int} requires a complete description of the time dependent probabilities of rotational states. A formulation of these statistics is developed below in which rotation rates about individual bonds are assumed to be independent.

Consider rotation about a single carbon-carbon bond located within a sequence of identical bonds. The rotational energy about this bond possesses a lowest minimum at $\phi = 0°$ for the planar form (tr). Two additional somewhat higher minima appear near 120° (g+) and 240° (g-). They lie at an energy approximately 0.5 kcal mole^{-1} above the trans minimum. Two equal maxima appear near 60° and 300°. The magnitude of these barriers is 3 to 4 kcal mole^{-1} above the trans zero energy position. Additionally, there is a high barrier near 180°. The height of this barrier, 9 to 10 kcal mole^{-1}, is so great as to be experimentally inaccessible. Such a barrier is sufficiently high to preclude the direct transition g+$\rightleftharpoons$g-. Transitions between rotational states therefore occur by passage over the two smaller barriers between trans and the two gauche states. Permitted transitions and their associated rates are described by

$$g- \underset{r_1}{\overset{r_2}{\rightleftharpoons}} tr \underset{r_2}{\overset{r_1}{\rightleftharpoons}} g+$$

The rates of transitions are assumed to be proportional to Boltzmann factors of the barrier heights. Values used here for calculations are $r_1 = (kT/h) \exp(-3/RT)$ and $r_2 = (kT/h) \exp(-2.5/RT)$, where h is Planck's constant.

If $p_{tr;j}(t)$ is the probability of rotational state trans for the j^{th} bond at time t, then a vector formed from such probabilities is defined by

$$\underset{\sim}{p}_j(t) = \begin{bmatrix} p_{tr;j}(t) \\ p_{g+;j}(t) \\ p_{g-;j}(t) \end{bmatrix} \tag{30}$$

The first order differential equation to describe the rates of transitions for this vector is

$$d\underset{\sim}{p}_j(t)/dt = \underset{\sim}{A}_j \underset{\sim}{p}_j(t) \tag{31}$$

The matrix $\underset{\sim}{A}$, expressed in terms of the transition rates r_1 and r_2, is

$$\underset{\sim}{A}_j = \begin{bmatrix} -2r_1 & r_2 & r_2 \\ r_1 & -r_2 & 0 \\ r_1 & 0 & -r_2 \end{bmatrix}, \qquad 2 < j < n-1 \tag{32}$$

The $-2r_1$ in the first element represents the rate and two directions in which the bond is permitted to turn away from trans. The gauche rotational states are only permitted to turn in the one direction toward trans; hence, the other diagonal terms are $-r_2$.

The solution to differential Equation 31 is

$$\underset{\sim}{p}_j(t) = \exp(\underset{\sim}{A}_j t)\ \underset{\sim}{p}_j(t=0) \tag{33}$$

Matrix $\underset{\sim}{A}_j$ can be diagonalized by a similarity transformation; hence

$$\underset{\sim}{B}_j^{-1} \underset{\sim}{A}_j \underset{\sim}{B}_j = \underset{\sim}{\Lambda}_j \tag{34}$$

B is a matrix formed from eigenvectors of A and Λ is the diagonal array of eigenvalues of A. Substitution of Equation 34 into Equation 33 yields

$$\underset{\sim}{p}_j(t) = \underset{\sim}{B}_j \exp(\underset{\sim}{\Lambda}_j t) \underset{\sim}{B}_j^{-1} \underset{\sim}{p}_j \quad (t=0) \tag{35}$$

For the vector and matrix in Equations 30 and 32, the solution in Equation 35 is given by the matrix depicted on page 115.

$$\underset{\sim}{p}_j(t) = \begin{bmatrix} p_{tr;j}(\infty) + [p_{g+;j}(\infty) + p_{g-;j}(\infty)]\, s_1 & p_{tr;j}(\infty)\,[1 - s_1] & p_{tr;j}(\infty)\,[1 - s_1] \\ p_{g+;j}(\infty)\,[1 - s_1] & p_{g+;j}(\infty) + (1/2)\, s_1 + [p_{tr;j}(\infty)/2]\, s_1 & p_{g+;j}(\infty) - (1/2)\, s_2 + [p_{tr;j}(\infty)/2]\, s_1 \\ p_{g-;j}(\infty)\,[1 - s_1] & p_{g-;j}(\infty) - (1/2)\, s_2 + [p_{tr;j}(\infty)/2]\, s_1 & p_{g-;j}(\infty) + (1/2)\, s_2 + [p_{tr;j}(\infty)/2]\, s_1 \end{bmatrix} \cdot \underset{\sim}{p}_j(0) \qquad (36)$$

The eigenrates are defined as $s_1 = \exp(-2r_1t-r_2t)$ and $s_2 = \exp(-r_2t)$.

If bond rotations are assumed to be independent of one another then this method may be extended to treat longer chains. The appropriate probability vector for a general n-bond chain will contain 3^{n-2} elements,

$$\underset{\sim}{p}^{(n)}(t) = \underset{\sim}{p}_2(t)\otimes\underset{\sim}{p}_3(t)\otimes\ldots\otimes\underset{\sim}{p}_j(t)\otimes\ldots\otimes\underset{\sim}{p}_{n-2}(t)\otimes\underset{\sim}{p}_{n-1}(t) \qquad (37)$$

The time derivative of Equation 37 is

$$\begin{aligned} d\underset{\sim}{p}^{(n)}/dt = {} & (d\underset{\sim}{p}_2/dt)\otimes\underset{\sim}{p}_3\otimes\ldots\otimes\underset{\sim}{p}_j\otimes\ldots\otimes\underset{\sim}{p}_{n-2}\otimes\underset{\sim}{p}_{n-1} \\ & + \underset{\sim}{p}_2\otimes(d\underset{\sim}{p}_3/dt)\otimes\ldots\otimes\underset{\sim}{p}_j\otimes\ldots\otimes\underset{\sim}{p}_{n-2}\otimes\underset{\sim}{p}_{n-1} \\ & \vdots \qquad\qquad\qquad\qquad\qquad \vdots \\ & + \underset{\sim}{p}_2\otimes\underset{\sim}{p}_3\otimes\ldots\otimes(d\underset{\sim}{p}_j/dt)\otimes\ldots\otimes\underset{\sim}{p}_{n-2}\otimes\underset{\sim}{p}_{n-1} \\ & \vdots \qquad\qquad\qquad\qquad\qquad \vdots \\ & + \underset{\sim}{p}_2\otimes\underset{\sim}{p}_3\otimes\ldots\otimes\underset{\sim}{p}_j\otimes\ldots\otimes(d\underset{\sim}{p}_{n-2}/dt)\otimes\underset{\sim}{p}_{n-1} \\ & + \underset{\sim}{p}_2\otimes\underset{\sim}{p}_3\otimes\ldots\otimes\underset{\sim}{p}_j\otimes\ldots\otimes\underset{\sim}{p}_{n-2}\otimes(d\underset{\sim}{p}_{n-1}/dt) \end{aligned} \qquad (38)$$

The explicit functional time dependence of the probabilities has been removed from Equation 38 and later equations. Unless otherwise stated, all probabilities to follow are for time t. Time derivatives on the right side of Equation 38 can be removed by substitution of Equation 31.

$$
\begin{aligned}
d\underset{\sim}{p}^{(n)}/dt = {} & \underset{\sim}{A}_2\underset{\sim}{p}_2 \circledast \underset{\sim}{p}_3 \circledast \ldots \circledast \underset{\sim}{p}_j \circledast \ldots \circledast \underset{\sim}{p}_{n-2} \circledast \underset{\sim}{p}_{n-1} \\
& + \underset{\sim}{p}_2 \circledast \underset{\sim}{A}_3\underset{\sim}{p}_3 \circledast \ldots \circledast \underset{\sim}{p}_j \circledast \ldots \circledast \underset{\sim}{p}_{n-2} \circledast \underset{\sim}{p}_{n-1} \\
& \quad \vdots \\
& + \underset{\sim}{p}_2 \circledast \underset{\sim}{p}_3 \circledast \ldots \circledast \underset{\sim}{A}_j\underset{\sim}{p}_j \circledast \ldots \circledast \underset{\sim}{p}_{n-2} \circledast \underset{\sim}{p}_{n-1} \\
& \quad \vdots \\
& + \underset{\sim}{p}_2 \circledast \underset{\sim}{p}_3 \circledast \ldots \circledast \underset{\sim}{p}_j \circledast \ldots \circledast \underset{\sim}{A}_{n-2}\underset{\sim}{p}_{n-2} \circledast \underset{\sim}{p}_{n-1} \\
& + \underset{\sim}{p}_2 \circledast \underset{\sim}{p}_3 \circledast \ldots \circledast \underset{\sim}{p}_j \circledast \ldots \circledast \underset{\sim}{p}_{n-2} \circledast \underset{\sim}{A}_{n-1}\underset{\sim}{p}_{n-1}
\end{aligned}
\tag{39}
$$

Matrices $\underset{\sim}{A}_j$ are given by Equation 32 except for $\underset{\sim}{A}_2$ and $\underset{\sim}{A}_{n-1}$ which are

$$
\underset{\sim}{A}_2 = \underset{\sim}{A}_{n-1} = \begin{bmatrix} -2r_1 & r_1 & r_1 \\ r_1 & -r_1 & 0 \\ r_1 & 0 & -r_1 \end{bmatrix}
$$

The direct product theorem for any arbitrary conformable matrices A, B, C and D permits the rearrangement $(AB) \circledast (CD) = (A \circledast C)(B \circledast D)$. Successive applications of this theorem to Equation 39 yields

$$\begin{aligned} d\underset{\sim}{p}^{(n)}/dt = [&(\underset{\sim}{A}_2 \otimes \underset{\sim}{I}_3 \otimes \ldots \otimes \underset{\sim}{I}_3 \otimes \ldots \otimes \underset{\sim}{I}_3 \otimes \underset{\sim}{I}_3) \\ &+ (\underset{\sim}{I}_3 \otimes \underset{\sim}{A}_3 \otimes \ldots \otimes \underset{\sim}{I}_3 \otimes \ldots \otimes \underset{\sim}{I}_3 \otimes \underset{\sim}{I}_3) \\ &\vdots \\ &+ (\underset{\sim}{I}_3 \otimes \underset{\sim}{I}_3 \otimes \ldots \otimes \underset{\sim}{A}_j \otimes \ldots \otimes \underset{\sim}{I}_3 \otimes \underset{\sim}{I}_3) \\ &\vdots \\ &+ (\underset{\sim}{I}_3 \otimes \underset{\sim}{I}_3 \otimes \ldots \otimes \underset{\sim}{I}_3 \otimes \ldots \otimes \underset{\sim}{A}_{n-2} \otimes \underset{\sim}{I}_3) \\ &+ (\underset{\sim}{I}_3 \otimes \underset{\sim}{I}_3 \otimes \ldots \otimes \underset{\sim}{I}_3 \otimes \ldots \otimes \underset{\sim}{I}_3 \otimes \underset{\sim}{A}_{n-1})] \; \underset{\sim}{p}^{(n)} \end{aligned} \tag{40}$$

Combination of terms on the right side of Equation 40 gives a result similar in form to Equation 31

$$d\underset{\sim}{p}^{(n)}/dt = \underset{\sim}{\mathcal{A}}\, \underset{\sim}{p}^{(n)} \tag{41}$$

Likewise, matrix $\underset{\sim}{\mathcal{A}}$ may be diagonalized and the solution expressed in a form similar to Equation 35,

$$\begin{aligned} \underset{\sim}{p}^{(n)} &= \underset{\sim}{\mathcal{B}} \exp(\mathcal{L}t)\, \underset{\sim}{\mathcal{B}}^{-1}\, \underset{\sim}{p}^{(n)}(t=0) \\ &= \underset{\sim}{\mathcal{C}}\, \underset{\sim}{p}^{(n)}(t=0) \end{aligned} \tag{42}$$

$\mathcal{B}$ is the matrix formed from eigenvectors of $\mathcal{A}$ and $\mathcal{L}$ is the diagonal array of eigenvalues of $\mathcal{A}$. Inspection of Equation 41 reveals that the matrix $\mathcal{A}$ has dimensions $3^{n-2} \times 3^{n-2}$. Practical computations with this method are therefore limited to $n \lesssim 7$. Another method (15) is more appropriate for treating longer chains.

Results of calculations above indicate that the effect of normal electric fields on rotational state probabilities is usually negligible. Hence, $\underset{\sim}{p}^{(n)}(t=0)$ in Equation 42 may be replaced with $\underset{\sim}{p}^{(n)}(t=\infty)$, the equilibrium value. In order to obtain the same

initial time values of $\mu^2(0)$ from both the partition function in Equation 8 and the statistics in Equation 42, the probability vector in Equation 37 is replaced for computational purposes with

$$\underset{\sim}{p}^{(n)}(t=0) = \begin{bmatrix} p_{tr,tr,\ldots,tr,tr} \\ p_{tr,tr,\ldots,tr,g+} \\ p_{tr,tr,\ldots,tr,g-} \\ p_{tr,tr,\ldots,g+,tr} \\ \vdots \\ p_{g-,g-,\ldots,g-,g+} \\ p_{g-,g-,\ldots,g-,g-} \end{bmatrix} \tag{43}$$

Each element of this vector represents the total equilibrium probability for an individual configuration. These probabilities may be calculated with the partition function in Equation 8. Neighbor dependence of the equilibrium statistics is thus reintroduced into Equation 42.

In order to reduce the sizes of matrices $\underset{\sim}{\mathcal{A}}$, the rows and columns corresponding to occurrence of g+g- and g-g+ pairs of states have been eliminated. Diagonal terms of $\underset{\sim}{\mathcal{A}}$ are adjusted appropriately to retain zero sums of each column. By this method, the dimensions of matrix $\underset{\sim}{\mathcal{A}}$ for n=6 are reduced from 81 x 81 to 41 x 41.

Matrix $\underset{\sim}{\mathcal{C}}$ in Equation 42 is composed of time conditional probabilities. The row indexes the configuration at time t and the column indexes the initial configuration. The total time dependent joint probability array is therefore given by

$$\underset{\sim}{\rho}^{(n)} = \underset{\sim}{\mathcal{C}}\,\mathrm{diag}[\underset{\sim}{p}^{(n)}(t=0)] \tag{44}$$

This matrix contains a complete description of the time dependence of the rotational state probabilities. The internal portion of the dipolar time correlation function is obtained by direct application of this matrix.

$$\Phi_{int} = \underset{\sim}{M}^T (\underset{\sim}{\mathcal{A}}^{(n)} \otimes \underset{\sim}{I}_3) \underset{\sim}{M} \tag{45}$$

Vector $\underset{\sim}{M}$ is formed from the dipole moment vectors for each chain configuration, calculated by Equation 4.

$$\underset{\sim}{M} = \begin{bmatrix} \mu_{tr,tr,\ldots,tr,tr} \\ \mu_{tr,tr,\ldots,tr,g+} \\ \cdot \\ \cdot \\ \cdot \\ \mu_{g-,g-,\ldots,g-,g-} \end{bmatrix} \tag{46}$$

Inspection of Equations 42 and 44 indicates that the internal dipolar time correlation function in Equation 45 may be expressed in the form

$$\Phi_{int} = \sum_j k_j \exp(\lambda_j t) \tag{47}$$

where λ_j is the j^{th} eigenrate from the diagonal array $\tilde{\mathcal{A}}$. The relative importance of eigenrates is shown in Figures 3 to 5 for chains of 4, 5 and 6 backbone bonds. The eigenrate is the inverse of the relaxation time; therefore, these diagrams are directly related to the distributions of relaxation times. With increasing chain length, additional relaxation times contribute to the correlation function. The mean relaxation time is shifted to shorter times for the longer chains. This is a consequence of the mechanism of independent relaxation about all chain bonds.

The total correlation function is expressed by

$$\Phi = \sum_j k_j \exp(\lambda_j' t) \tag{48}$$

where $\lambda_j' = \lambda_j - 1/\tau_{rot}$. The effect of including this independent external rotation is to shift all internal rates by the same amount. Approximate values of τ_{rot} were chosen from the results of Rayleigh scattering experiments for the similar liquid alkyl bromides (16). Use of empirical equations given in Reference 16 for the chain length and temperature dependences of the orientational relaxation times yields the values presented in Table II. These values for the monobromo compounds are substituted for the values required for the dibromo compounds with the same number of carbon atoms. It is assumed that introduction of the additional bromine atom does not significantly change the rotational diffusion rate. The magnitude of the error introduced by assuming that the two experimental methods yield the same relaxation time depends upon the chain length. Estimates (16) of this error indicate that it is probably less than 50%.

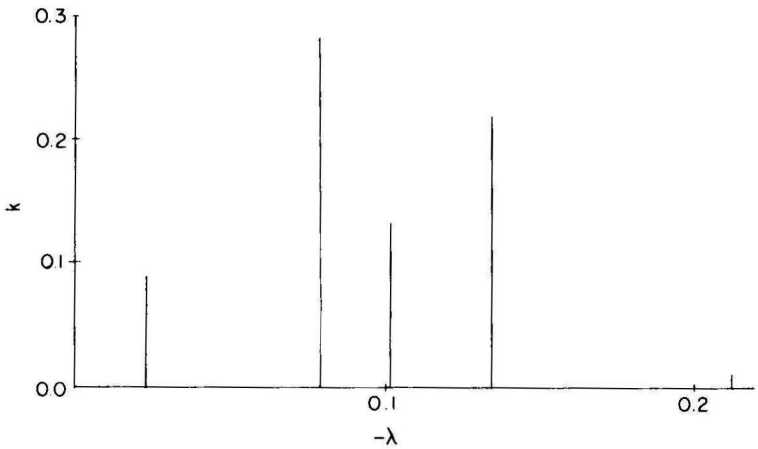

Figure 3. Contributions k of eigenrates λ to Φ_{int}, the normalized internal dipolar correlation function, for 1,3-dibromo-n-propane at 25°. Units of λ are 10^{12} sec^{-1}.

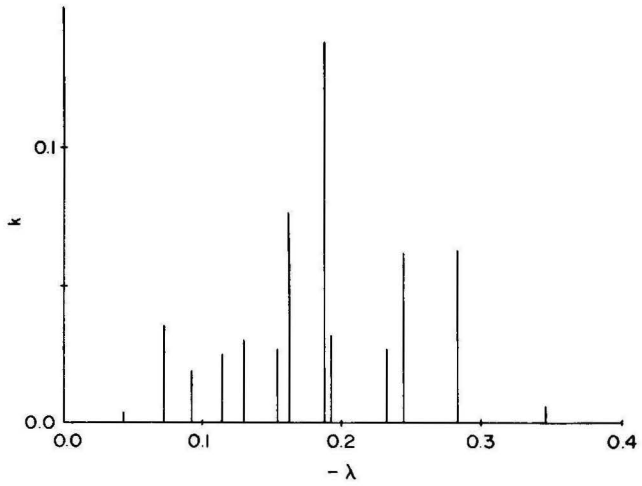

Figure 4. Contributions k of eigenrates λ to Φ_{int}, the normalized internal dipolar correlation function, for 1,4-dibromo-n-butane at 25°. Units of λ are 10^{12} sec^{-1}.

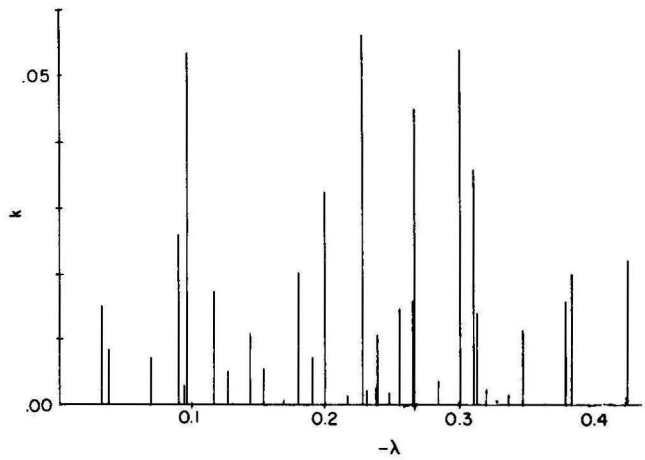

Figure 5. Contributions k of eigenrates λ to Φ_{int}, the normalized internal dipolar correlation function, for 1,5-dibromo-n-pentane at 25°. Units of λ are 10^{12} sec^{-1}.

TABLE II

Orientational Relaxation Times from Rayleigh Scattering Experiments (16)

Liquid	Temperature	τ_{rot} x 10^{12} (sec)
1-propyl bromide	25°	3.4
1-butyl bromide	0°	8.0
1-butyl bromide	25°	5.8
1-butyl bromide	50°	4.7
1-pentyl bromide	25°	9.9

A correlation time for the normalized total correlation function in Equation 48 is defined by

$$\tau_c = \int_o^\infty \Phi \, dt$$

$$= \sum_j \int_o^\infty k_j \exp(\lambda_j' t) \, dt \qquad (49)$$

Integration of this equation yields

$$\tau_c = - \sum k_j / \lambda_j'$$

Values of τ_c calculated at 25° for the α,ω-dibromo-n-alkanes are 2.84 x 10^{-12} sec for n = 4, 4.22 x 10^{-12} sec for n = 5 and 6.41 x 10^{-12} sec for n = 6.

Figure 6 displays the decay of the total correlation function at 25° for n = 4 to 6. The smallest molecule relaxes fastest only because the smallest values of τ_{rot} were used. If the same value of external relaxation time had been used for all chain lengths, then the curves would appear in the opposite order. The reason for this behavior is that longer chains in this model manifest shorter mean internal relaxation times.

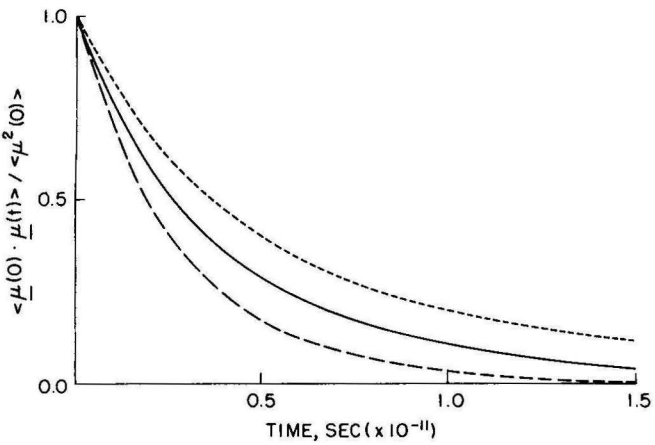

Figure 6. Time decay of total normalized dipolar time correlation function at 25°. Upper curve represents behavior for a chain length n=6. Middle curve is for n=5 and lowest curve is for n=4.

DIELECTRIC CONSTANT

The complex dielectric constant ε^* is directly proportional to the Laplace transform L of the time derivative of the total dipolar correlation function.

$$(\varepsilon^*-\varepsilon_\infty)/(\varepsilon_o-\varepsilon_\infty) = L(-d\Phi/dt) \tag{51}$$

ε_o and ε_∞ are respectively the static and infinite frequency dielectric constants. Substitution for the argument of the Laplace transform from Equation 48 yields

$$(\varepsilon^*-\varepsilon_\infty)/(\varepsilon_o-\varepsilon_\infty) = -\sum_j \lambda_j' k_j L[\exp(\lambda_j' t)] \tag{52}$$

Evaluation of the Laplace transform gives

$$(\varepsilon^*-\varepsilon_\infty)/(\varepsilon_o-\varepsilon_\infty) = -\sum_j \lambda_j' k_j/(i\omega-\lambda_j') \qquad (53)$$

where ω is identified with frequency. If $-\lambda_j$ is expressed as the inverse of relaxation time τ_j, then the real part of the dielectric constant is given by

$$(\varepsilon'-\varepsilon_\infty)/(\varepsilon_o-\varepsilon_\infty) = \sum_j k_j/(1+\omega^2\tau_j^2) \qquad (54)$$

The imaginary part of the dielectric constant is

$$\varepsilon''/(\varepsilon_o-\varepsilon_\infty) = \sum_j k_j\omega\tau_j/(1+\omega^2\tau_j^2) \qquad (55)$$

Each term of the series in Equations 54 and 55 is identical to the result for the Debye one relaxation time model. The dielectric constant for the present model is given by a sum of these Debye-like terms. If the real part for the Debye model is plotted on one axis and the imaginary part on the other axis, the familiar Cole-Cole semicircle is obtained. The results of such plots are displayed in Figure 7 for the chains with n = 4, 5 and 6. The uppermost curve for 1,3-dibromo-n-propane is indistinguishable from the one relaxation semicircle. Curves for longer chains are depressed and slightly skewed from this limit. Such depressions and high frequency broadening is commonly observed for systems with multiple relaxation times. These deviations in Figure 7 are direct results of the distributions of relaxation rates depicted in Figures 3 - 5.

The temperature dependence of the real and imaginary dielectric constant for $Br-(CH_2)_4-Br$ is presented in Figures 8 and 9. Temperature affects the value of τ_{rot} chosen from Table II as well as the Boltzmann factors for rates of passage over barriers and for equilibrium statistical weights of rotational isomers. At higher temperatures the dispersion region is shifted to higher frequencies.

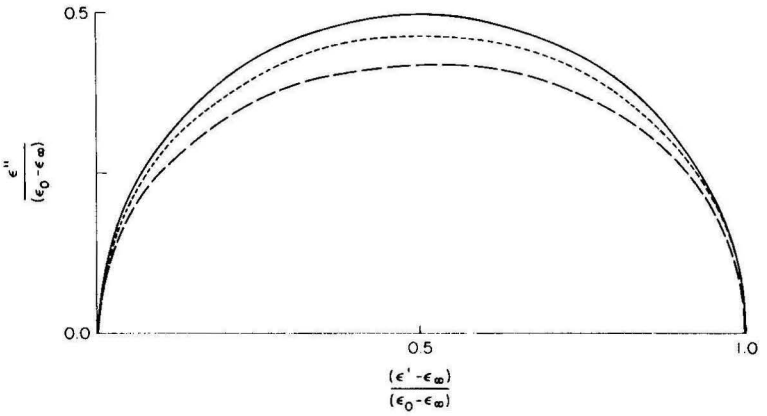

Figure 7. Cole-Cole diagram of dielectric behavior. Ordinate represents the imaginary part of the dielectric constant, and the abscissa is the real part. Upper curve is the Debye one relaxation time semicircle. The depressed curve of short dashes is for 1,4-dibromo-n-butane. Curve of long dashes represents behavior of 1,5-dibromopentane. All calculated curves are for 25°.

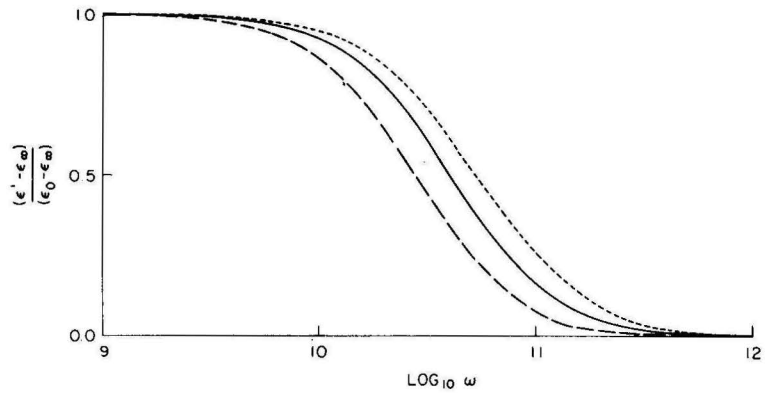

Figure 8. Frequency dependence of real part of dielectric constant for 1,4-dibromo-n-butane at three temperatures. Curve of small dashes is for 50°; solid curve is for 25°; long dash curve is for 0°.

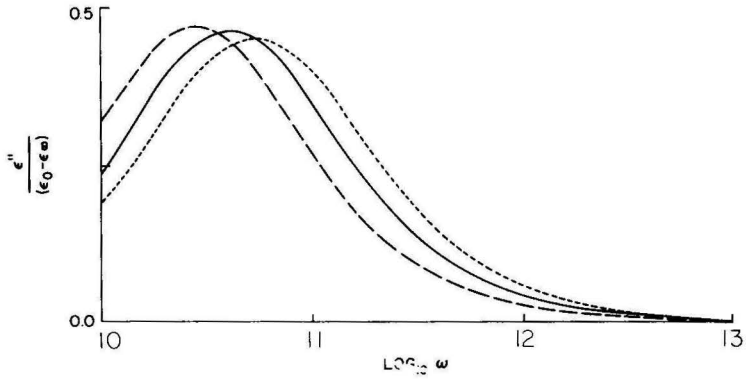

Figure 9. Frequency dependence of imaginary part of dielectric constant for 1,4-dibromo-n-butane at three temperatures. Curves are designated as in Figure 8.

The present theory has been developed for isolated molecules. Any comparison of these calculated results with experiment would require consideration of interactions with the surrounding medium. Numerous approximate theories (9-13) for this purpose exist. However, unavailability of experiments in the very high frequency range of simple configurational transitions does not encourage further pursuit. A preliminary estimate of the effect of intermolecular interactions in the pure liquids was performed by the method of References 12 and 13. The deviations from the Debye model manifested in Figure 7 were considerably reduced.

The present method for short chains admits of extension to more complex configurational transition schemes. Simultaneous transitions about several bonds may be accommodated by modifying matrix Q in Equation 41 to include additional non-zero terms. In this manner any desired motions, such as the so-called crankshaft motion, may be included. The range of bonds encompassed by such motions is limited only because this method is limited to short chains. Also, it is possible to treat relaxation properties of other molecules (4,17) using this model, if their structural features are known.

The model presented is a first attempt to account for the effect of detailed structural features on non-equilibrium properties. It may be appropriately applied only in the case of small deviations from equilibrium. Account has not been taken of large non-equilibrium effects such as bond length distortions and significant distortions of bond angles. However, such effects are not expected to be important for the application of small external fields. In its present application, transitions about all bonds have been assumed to occur independently and at the same rate. Frictional resistance to motions will modify transition rates. These modifications will show dependence on both chain length and configuration. For example, in a viscous medium it is more difficult to rotate about a bond in the middle of a long chain than about a terminal bond. The present isolated molecule theory accounts for neither hydrodynamic nor electrical intermolecular interactions.

ACKNOWLEDGMENT

The author wishes to thank B. H. Zimm and G. H. Weiss for helpful discussions

REFERENCES

1. P. E. Rouse, Jr., J. Chem. Phys. 21, 1272 (1953).
2. B. H. Zimm, J. Chem. Phys. 24, 269 (1956).
3. M. V. Volkenstein, CONFIGURATIONAL STATISTICS OF POLYMERIC CHAINS, Interscience, New York, 1963.
4. P. J. Flory, STATISTICAL MECHANICS OF CHAIN MOLECULES, Interscience, New York, 1969.
5. W. J. Leonard, Jr., R. L. Jernigan and P. J. Flory, J. Chem. Phys. 43, 2256 (1965).
6. A. Abe, R. L. Jernigan and P. J. Flory, J. Am. Chem. Soc. 88, 631 (1966).
7. P. J. Flory and R. L. Jernigan, J. Chem. Phys. 42, 3509 (1965).
8. Y. Abe and P. J. Flory, J. Chem. Phys. 52, 2814 (1970).
9. R. H. Cole, J. Chem. Phys. 42, 637 (1965).
10. S. H. Glarum, J. Chem. Phys. 33, 1371 (1960).
11. E. Fatuzzo and P. R. Mason, Proc. Phys. Soc. 90, 741 (1967).
12. D. D. Klug, D. E. Kranbuehl and W. E. Vaughan, J. Chem. Phys. 50, 3904 (1969).
13. J.-L. Rivail, J. Chim. Phys. 66, 981 (1969).
14. See, for example, J. D. Hoffman and H. G. Pfeiffer, J. Chem. Phys. 22, 132 (1954).
15. R. L. Jernigan, to be published.
16. D. A. Pinnow, S. J. Candau and T. A. Litovitz, J. Chem. Phys. 49, 347 (1968).
17. T. W. Bates and W. H. Stockmayer, Macromolecules 1, 12 (1968).